

# Vortex rings and global hyperon polarization at the NICA energies

N.S. Tsegelnik<sup>a</sup>, E.E. Kolomeitsev<sup>a,b</sup>, and V.V. Voronyuk<sup>a,c</sup>

<sup>a</sup>JINR, Dubna, Russia

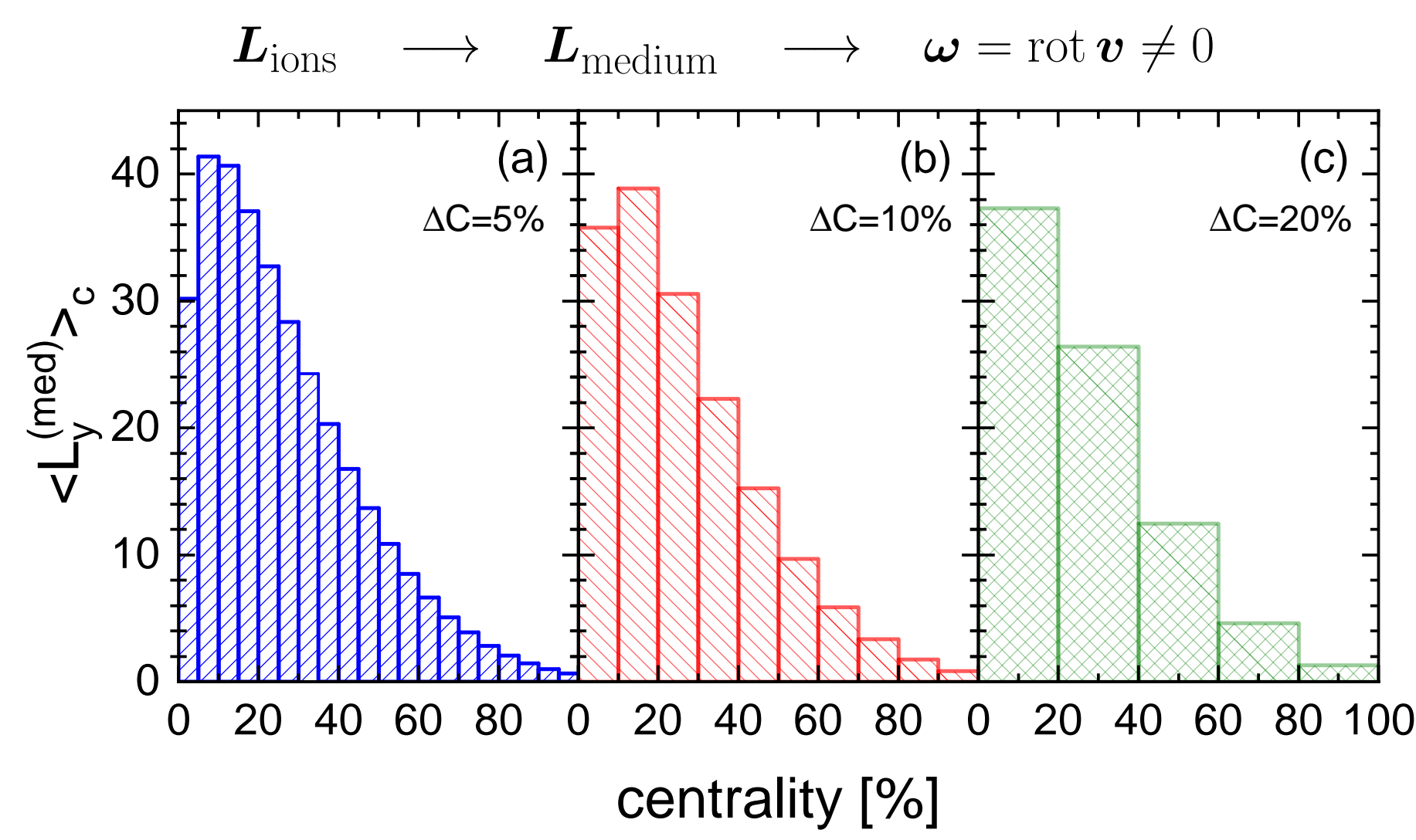
<sup>b</sup>MBU, Banska Bystrica, Slovakia

<sup>c</sup>BITP, Kiev, Ukraine



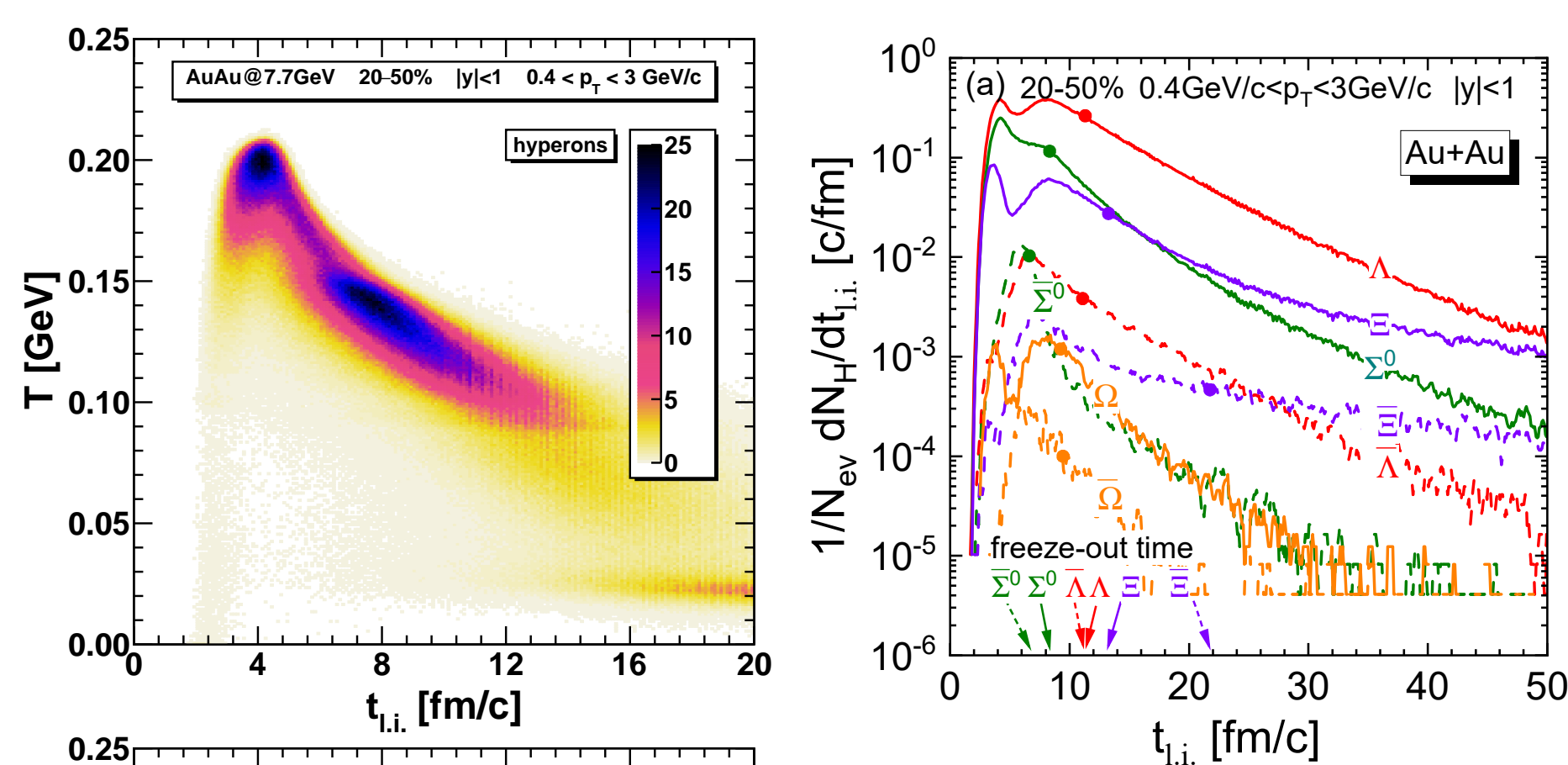
## 1. Introduction

- Hot and dense created matter undergoes explosive expansion.
- Angular momentum of ions  $\rightarrow$  medium  $\rightarrow$  **vorticity**



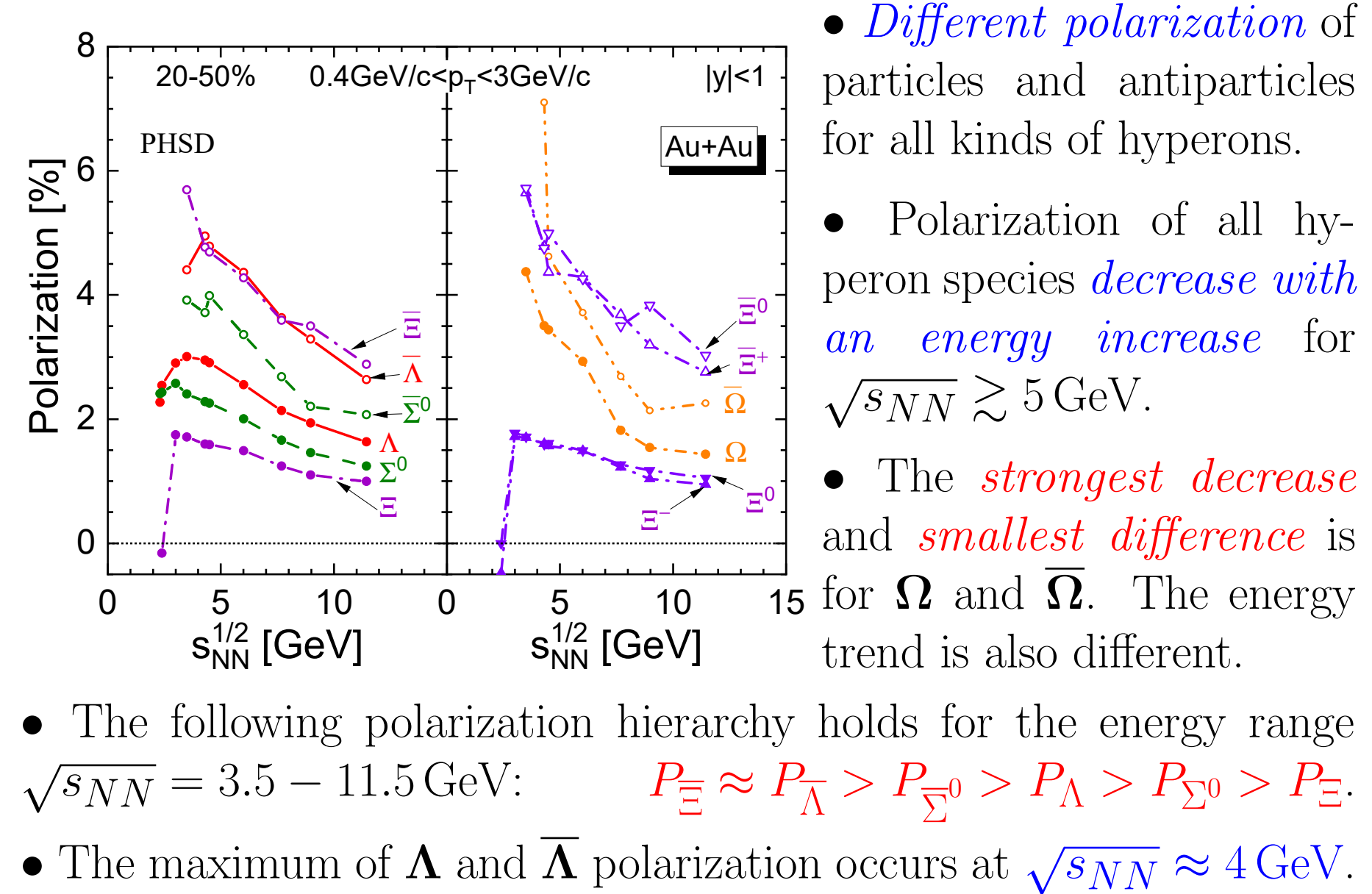
- Vorticity  $\rightarrow$  **spin polarization** [1]  $\leftrightarrow \langle P_{\Lambda} \rangle \approx \text{rot} \left( \frac{\mathbf{v}}{4T} \right) \approx \frac{\omega}{4T}$
- The  $\mathbf{P}$ -violation in weak decays  $\rightarrow$  the angular distribution of final protons depends on the orientation of the  $\Lambda$ -hyperons spin.
- Nonzero global polarization measured by STAR [2], HADES [3].

## 4. Freeze-out conditions [9, 10]



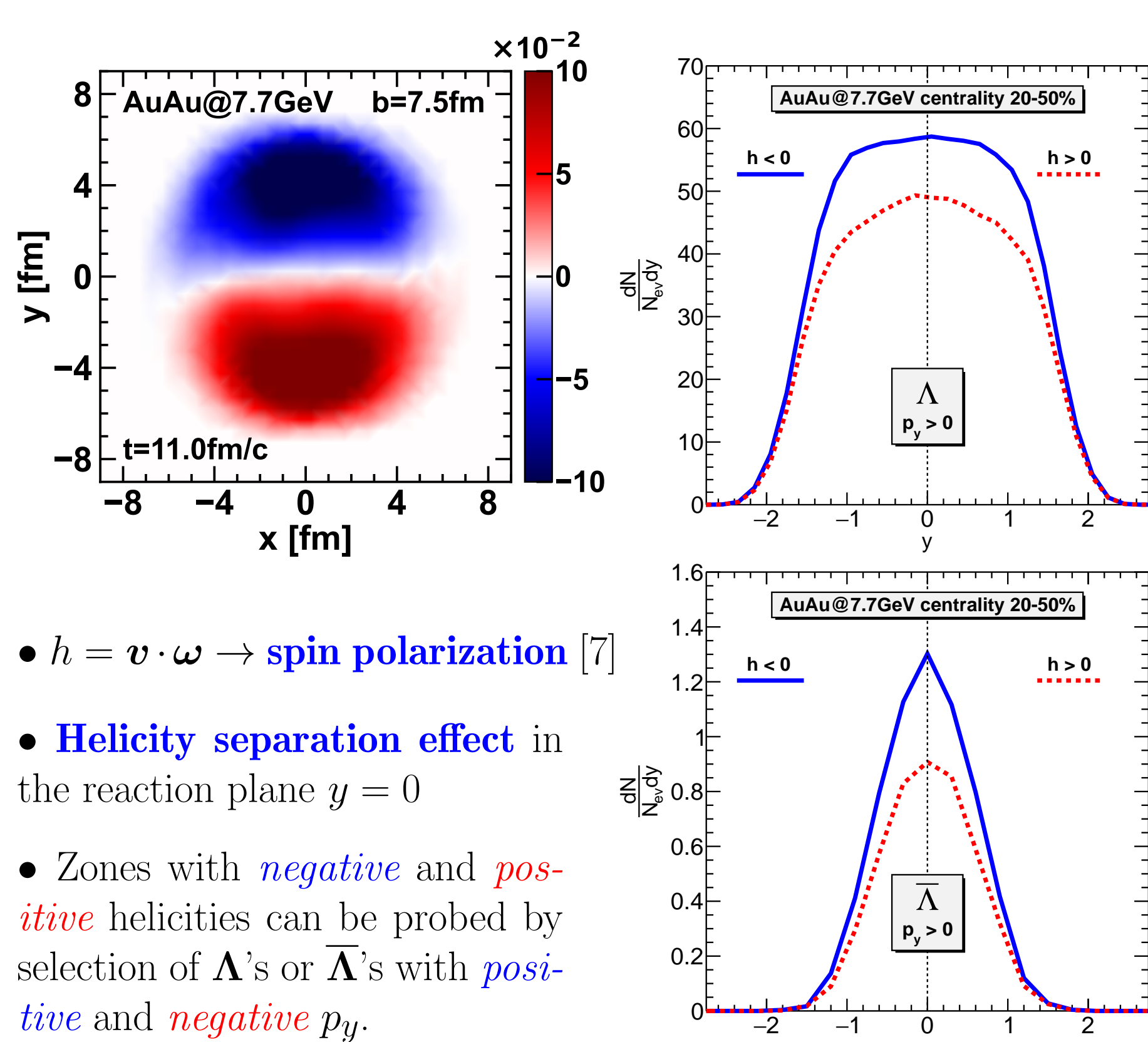
- Two main sources for **hyperons** and only **one** for **antihyperons**.
- Different thermodynamic conditions for particles and antiparticles  $\rightarrow$  **different polarization!**
- $t_{\Lambda}^{(f.o.)} \approx t_{\bar{\Lambda}}^{(f.o.)}$ ,  $t_{\Sigma}^{(f.o.)} \approx t_{\bar{\Sigma}}^{(f.o.)}$
- $t_{\Sigma}^{(f.o.)} > t_{\bar{\Sigma}}^{(f.o.)}$ ,  $t_{\Xi}^{(f.o.)} < t_{\bar{\Xi}}^{(f.o.)}$

## 6. Hyperon species polarization [10]



- Different polarization of particles and antiparticles for all kinds of hyperons.
- Polarization of all hyperon species **decrease with an energy increase** for  $\sqrt{s_{NN}} \gtrsim 5$  GeV.
- The **strongest decrease** and **smallest difference** is for  $\Omega$  and  $\bar{\Omega}$ . The energy trend is also different.
- The following polarization hierarchy holds for the energy range  $\sqrt{s_{NN}} = 3.5 - 11.5$  GeV:  $P_{\Xi} \approx P_{\bar{\Xi}} > P_{\Sigma^0} > P_{\Lambda} > P_{\Sigma^-} > P_{\Xi^-}$ .
- The maximum of  $\Lambda$  and  $\bar{\Lambda}$  polarization occurs at  $\sqrt{s_{NN}} \approx 4$  GeV.

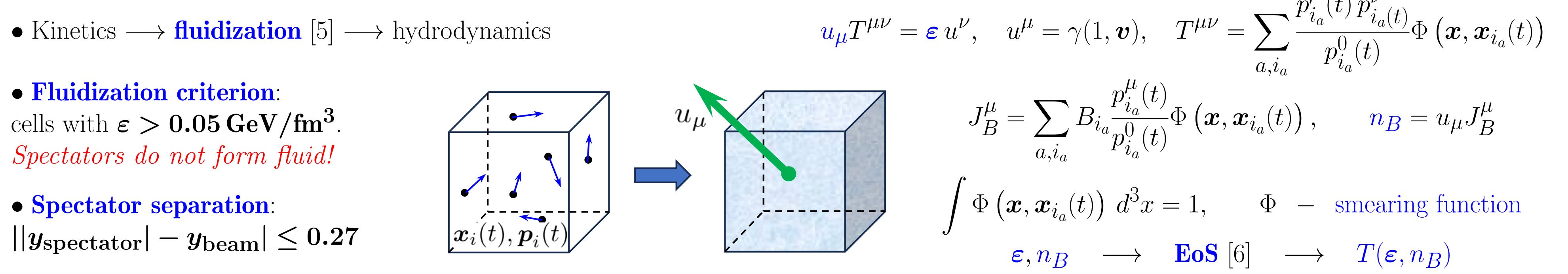
## 8. Hydrodynamic helicity [5]



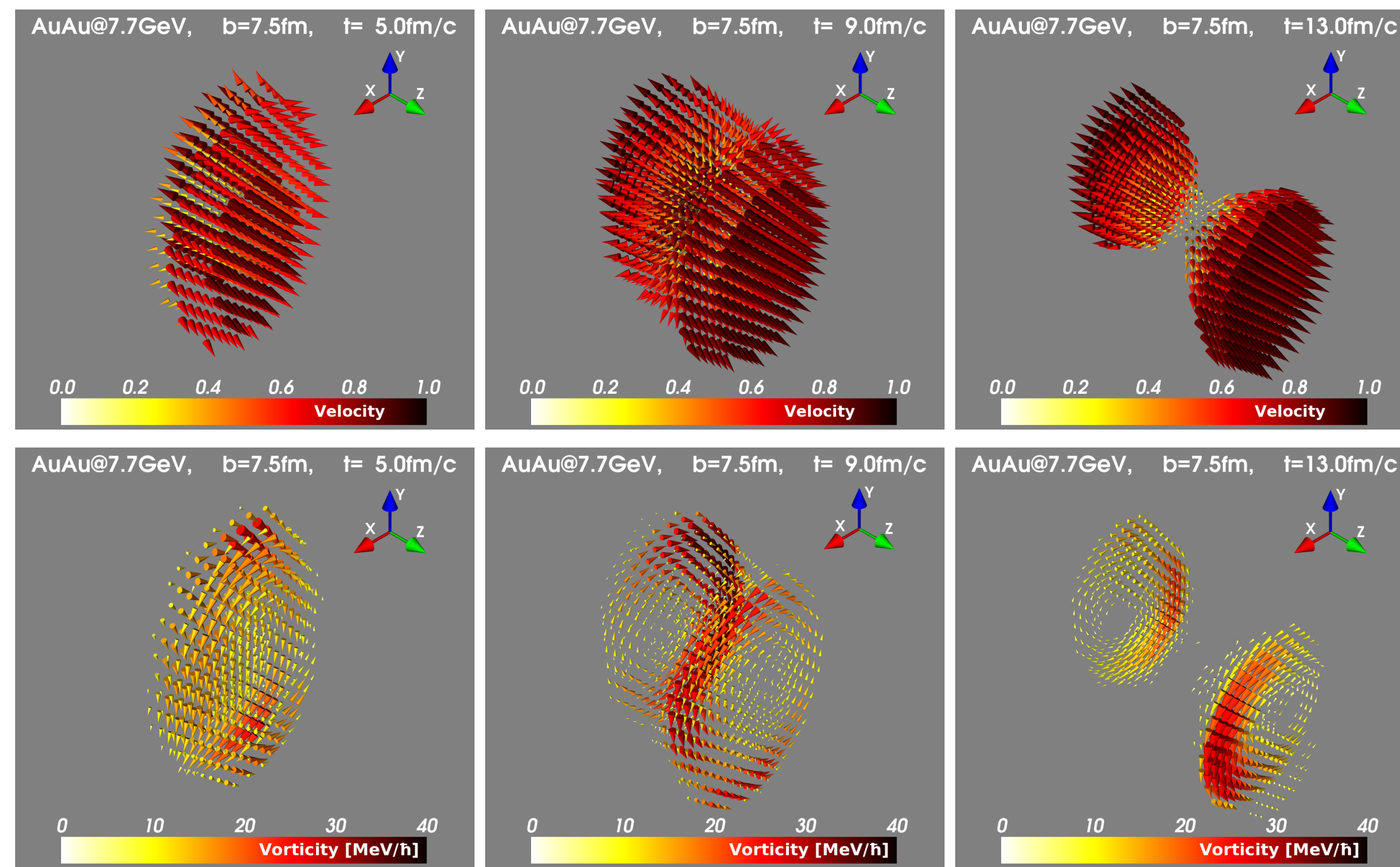
- $h = \mathbf{v} \cdot \boldsymbol{\omega} \rightarrow$  **spin polarization** [7]
- Helicity separation effect** in the reaction plane  $y = 0$
- Zones with **negative** and **positive** helicities can be probed by selection of  $\Lambda$ 's or  $\bar{\Lambda}$ 's with **positive** and **negative**  $p_y$ .

## 2. Setup

- The **Parton-Hadron-String Dynamic** model [4]: *the generalized off-shell transport equations*, **Dynamical Quasi-Particle Model** (for partons), **FRITIOF Lund** (strings breaking) **PYTHIA** and **JETSET** (jet production and fragmentation), **Chiral Symmetry Restoration**, ...

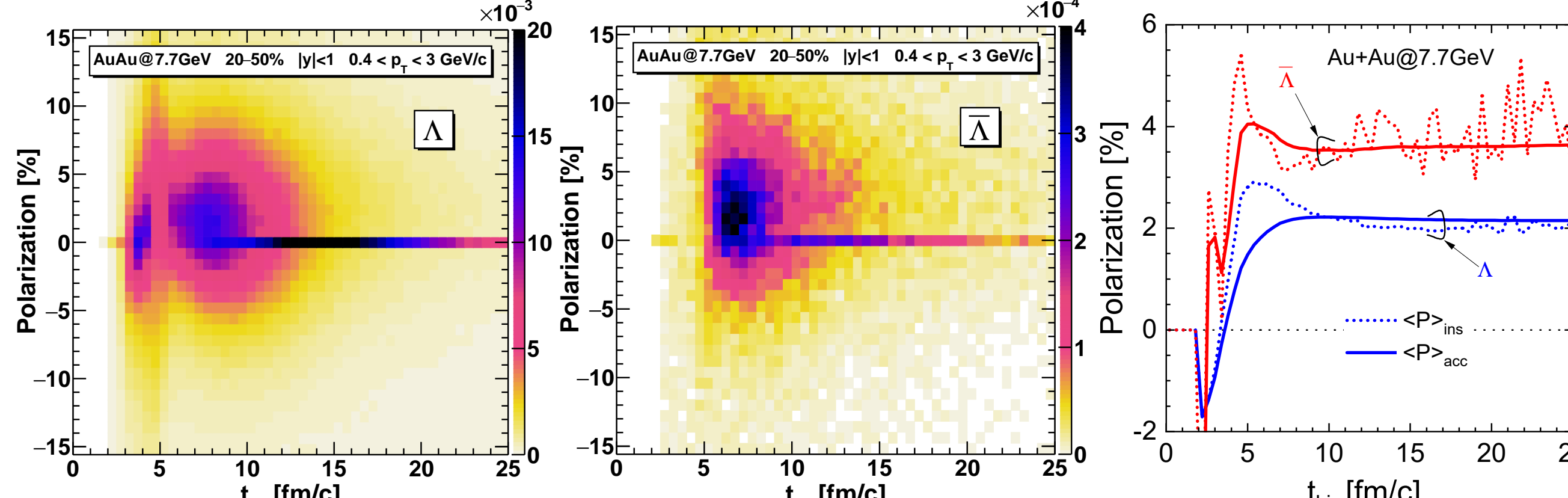


## 3. Velocity and vorticity fields [5, 9]



- The fireball velocity consist of the **irrotational (2+1)D Hubble-like** and **rotational** terms.
- Maximum of the vorticity is located **at the edges of the system**.
- Two deformed **elliptical vortex rings** move and rotate in opposite directions along the collision axis.
- The ring deformation depends on the impact parameter.
- In other works the **vortex sheets** [7], **vortex rings** [8] were predicted.

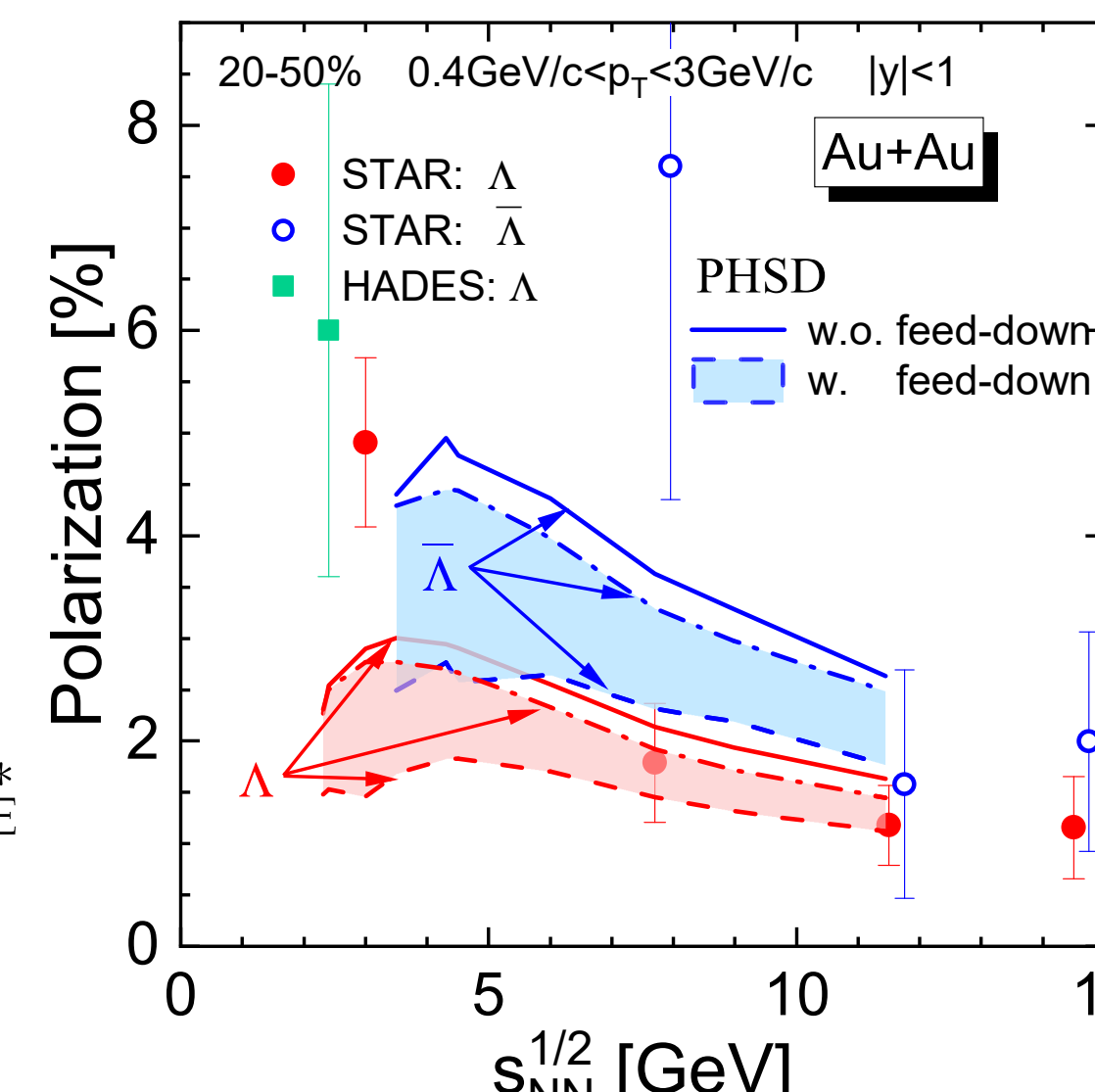
## 5. Polarization source [9, 10]



- Two main sources for  $\Lambda$  and only **one** for  $\bar{\Lambda}$ .
- The following relation holds for both instantaneous and accumulated polarizations for  $t_{li} \gtrsim 3$  fm/c:  $P_y(\bar{\Lambda}) > P_y(\Lambda)$
- For  $t \gtrsim 10$  fm/c the accumulated polarization stays **approximately constant**.
- Change in the polarization sign at the moment of full overlap.

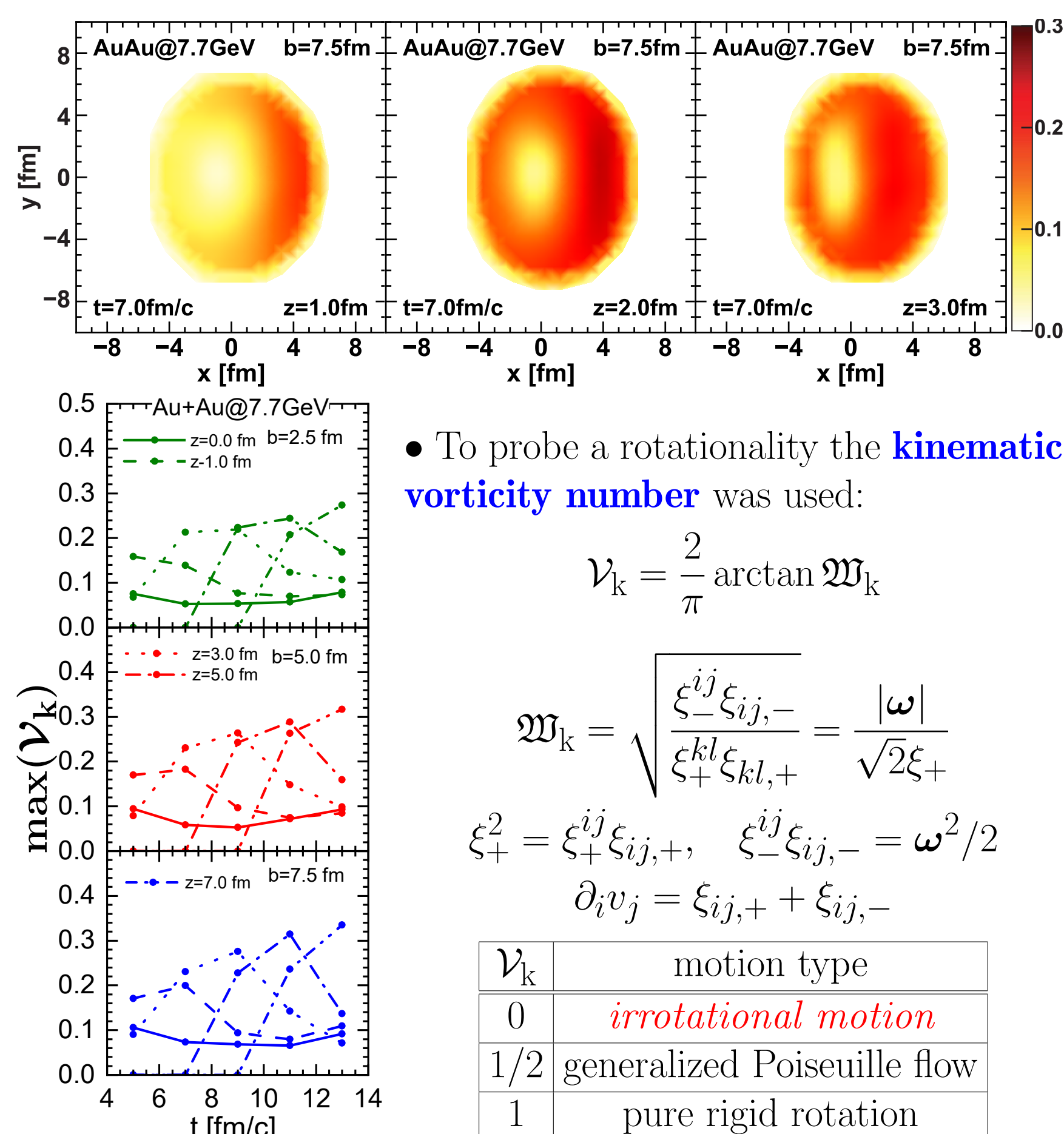
## 7. Feed-down effects [10]

- The feed-down contributions:
- strong** decays are already included
- weak** decays:  $\Xi \rightarrow \Lambda + \pi$ , contribution from  $\Omega$  is negligible
- electromagnetic** decays:  $\Sigma \rightarrow \Lambda + \gamma$
- The total measured spin vector for  $\Lambda(\bar{\Lambda})$ :  
 $S_{\Lambda}^{*(\text{meas})} = S_{\Lambda}^{*(\text{prim})} + S_{\Lambda}^{*(\Sigma^0)} + S_{\Lambda}^{*(\Xi)}$   
 $S_{\Lambda}^{*(\Sigma^0)} = f_{\Lambda\Sigma^0} C_{\Lambda\Sigma^0} S_{\Sigma^0}^*$ ,  $S_{\Lambda}^{*(\Xi)} = f_{\Lambda\Xi} C_{\Lambda\Xi} S_{\Xi}^*$   
 $f_{H\Lambda} = N_H / (N_H + N_{H'})$ ,  $B_{\Lambda\Xi} = 0.995$   
 $C_{\Lambda\Sigma^0} = -1/3$ ,  $C_{\Lambda\Xi^0} = 0.914$ ,  $C_{\Lambda\Xi^-} = 0.943$



- Polarization of the  $\Lambda$  hyperons **agrees** with experimental data, except low energies  $\sqrt{s_{NN}} \leq 3$  GeV. The **maximum** of the  $\Lambda$  polarization at  $\sqrt{s_{NN}} \approx 4$  GeV.
- Polarization of  $\bar{\Lambda}$  **larger** in 1.5 - 2 times than  $\Lambda$ . It **agrees** with experimental data at  $\sqrt{s_{NN}} = 11.5$  GeV, but is **less** at  $\sqrt{s_{NN}} = 7.7$  GeV.
- The relationship between the multiplicities of  $\Lambda$  and  $\Sigma$  hyperons is unknown, so the filled area in the figure corresponds to their different proportions.
- Strong polarization suppression is caused by the **feed-down from  $\Sigma^0$  and  $\Xi^0$**  hyperons.

## 9. Measure of rotationality [5]



- To probe a rotationality the **kinematic vorticity number** was used:  
 $\mathcal{V}_k = \frac{2}{\pi} \arctan \mathfrak{W}_k$   
 $\mathfrak{W}_k = \frac{\xi_{-}^{ij} \xi_{ij,-}}{\xi_{+}^{kl} \xi_{kl,+}} = \frac{|\omega|}{\sqrt{2}\xi_{+}}$   
 $\xi_{+}^2 = \xi_{+}^{ij} \xi_{ij,+}$ ,  $\xi_{-}^2 = \xi_{-}^{ij} \xi_{ij,-} = \omega^2 / 2$   
 $\partial_i v_j = \xi_{ij,+} + \xi_{ij,-}$

$\mathcal{V}_k$	motion type
0	irrotational motion
1/2	generalized Poiseuille flow
1	pure rigid rotation

## 10. Summary

- The (2+1)D Hubble-like expansion + vorticity at the system edges  $\leftrightarrow$  two deformed elliptical vortex rings.
- Different polarization of particles and antiparticles for all hyperons.
- The difference in polarizations arises naturally and can be related to the difference in the thermodynamic conditions and vorticity field.
- Strong polarization suppression due to the feed-down from  $\Sigma^0$  ( $\Xi^0$ ).
- The helicity separation effect in the reaction plane.
- The motion does not reach the Poiseuille flow and is close to the pure shear deformation.

## References

- [1] F. Becattini, V. Chandra, L. Del Zanna, and E. Grossi, Ann. Phys. (NY) **338**, 32 (2013).
- [2] L. Adamczyk et al. (STAR Collaboration), Nature **548**, 62 (2017).
- [3] R.A. Yassine et al. (HADES Collaboration), Phys. Lett. B **835** (2022) 137506.
- [4] W. Cassing, E. L. Bratkovskaya, Nucl. Phys. A **831**, 215 (2009).
- [5] N.S. Tsegelnik, E.E. Kolomeitsev, V. Voronyuk, Phys. Rev. C **107**, 034906 (2023).
- [6] L.M. Satarov, M.N. Dmitriev, and I.N. Mishustin, Phys. At. Nucl. **72**, 1390 (2009).
- [7] M.I. Baznat, K.K. Gudima, A.S. Sorin, and O.V. Teryaev, Phys. Rev. C **93**, 031902 (2016).
- [8] Yu.B. Ivanov and A.A. Soldatov, Phys. Rev. C **97**, 044915 (2018).
- [9] N.S. Tsegelnik, E.E. Kolomeitsev, V. Voronyuk, Particles **2023**, 373 (2023).
- [10] V. Voronyuk, E.E. Kolomeitsev, N.S. Tsegelnik, arXiv:2305.10792 [nucl-th].